Supporting Information for

A zinc metal complex as an NIR emissive probe for real-time dynamics and *in vivo* embryogenic evolution of lysosomes using super-resolution microscopy

*Abdul Salam[1,ξ], Kush Kaushik[1,ξ], Bodhidipra Mukherjee[2,ξ], Farhan Anjum[2], Goraksha T. Sapkal[1], Shagun Sharma[1], Richa Garg[1] and Chayan Kanti Nandi[1,2]**

[1]School of Chemical Sciences, Indian Institute of Technology Mandi, H.P.-175075, India

[2]School of Biosciences and Bioengineering, Indian Institute of Technology Mandi, H.P.-175075, India

[ξ]Abdul Salam, Kush Kaushik and Bodhidipra Mukherjee equally contributed to this work

EXPERIMENTAL SECTION

Materials

All the commercially available reagents were purchased and used without further purification, including morpholine, zinc acetate dihydrate, 3-nitrophenol, methyl iodide, anhydrous tin chloride, BBr_3, 1,3-dibromopropane. Experiments were conducted under an atmosphere of dry nitrogen. All solvents were of spectral grade unless otherwise noted. Liquid column chromatography was performed over silica gel (Merck Silica Gel 60-120 mesh, 100-200 mesh). Developed TLC plates were visualized under a short-wave UV lamp.

Characterization

Nuclear magnetic resonance spectroscopy

The ^{1}H and ^{13}C NMR spectroscopic measurements were carried out using a Jeol JNM ECX-500 NMR spectrometer at 500 MHz with tetramethylsilane (TMS) as an internal reference; ^{1}H (referenced to TMS at $\delta = 0.0$ ppm), and ^{13}C (referenced to $CDCl_3$ at $\delta = 77.16$ ppm. Chemical shifts of ^{1}H and ^{13}C spectra were interpreted with the support of ChemDraw 20.1.1. High-resolution electrospray ionization (ESI) mass spectra were recorded on a Bruker impact-HD spectrometer with a quadrupole time-of-flight mass analyzer.

UV-visible and steady-state fluorescence

The UV-visible spectra of the Zn-complex was recorded on a Shimadzu UV-Vis 2450 spectrophotometer using a 10 mm path-length quartz cuvette. The Agilent Cary eclipse fluorescence spectrometer was used to record the steady-state fluorescence.

Fluorescence lifetime spectroscopy

The fluorescence lifetime decays were assessed using the Horiba scientific Delta Flex TCSPC system with Pulsed LED Sources. 570 nm pulsed NanoLED source was used for excitation. For spectral value deconvolution, Ludox has been employed for measuring the instrument response function (IRF). Data acquisition was performed using Data station software and data was fitted using DAS6 analysis software from Horiba.

Quantum yield

The relative quantum yield of the Zn-complex was calculated using an optically matching solution of Rhodamine B in ethanol ($\varphi = 0.9$) as a reference. The optical density of Zn-complex and Rhodamine B was less than 0.1. The values of fluorescence quantum yield, φ (sample), were calculated by using the following equation:

$$\varphi_S = \varphi_R \frac{Grad_S}{Grad_R} \times \frac{{\eta^2}_S}{{\eta^2}_R}$$

Where the subscript 'S' and 'R' denote the sample and reference respectively, φ is the quantum yield, Grad is the gradient from the plot of integrated fluorescence intensity vs absorbance, and η is the refractive index of pure solvents.

Cleaning of glass coverslip

For single-molecule fluorescence studies, glass coverslips cannot be cleaned in a normal manner as ultra-high purity is needed for the same. 100 mL of piranha solution with a 3:1 ratio of H_2SO_4:H_2O_2 was prepared freshly. 25-30 glass coverslips were added individually to the freshly prepared piranha solution with slight shaking. Slides were kept in piranha solution for 0.5 h to 1 h. Then the acid was discarded and the coverslips were rinsed with deionized water for 3-4 times. Slides were then sonicated for 15minutes and again the coverslips were rinsed with deionized water for 3-4 times. These steps were repeated for 4 times and then the coverslips were used for further single-molecule fluorescence studies.

Single-molecule fluorescence spectroscopy

Zn-complex was spin-coated on a pre-cleaned glass coverslip to acquire single-molecule time traces. A 532 nm diode laser with 50 mW maximum power was used to excite the sample. The emission of Zn-complex was collected using a 600/50 nm filter set. An oil immersion Nikon TIRF objective (100x magnification and 1.49 NA) was mounted on a custom-built inverted optical microscope. A 560 nm high pass Dichroic (AHF Analysentechnik) was used to differentiate the excitation and emission light. Andor EMCCD iXon Ultra was used to record the single molecule emission videos with an exposure time of 50 ms. The EMCCD camera was set to an EM-gain of 300, a pixel readout rate of 17 MHz, and had both frame transfer and photon counting modes activated. The fluorescence from single molecules created diffraction-limited spots that were visible during observation. These videos were documented using Andor Solis Software. The EMCCD converted incident photons into electrons, which were then quantified as digital counts. These photon counts were reverse-calculated to account for the instrument's settings, including EM gain, Pre-amplifier gain, and the count values, utilizing the photon counting mode of the instrument. Scripts written in MATLAB were employed to pinpoint single molecules and extract data such as total photon counts, photons per cycle, and temporal traces. The movies, recorded in the kinetic mode of the EMCCD, provided time/frame trajectories for the counts/intensity at specific pixels over the set exposure time. These trajectories were preserved for subsequent analysis.

Localization precision

Localization precision (σ_{SMLM}) was obtained with the help of the ThunderSTORM plugin of ImageJ. Nearly 5000 frames were recorded for Zn-complex and analyzed with the default settings of ThunderSTORM. The table containing information on localization (the x, y coordinates for each particle from each frame) was obtained. Around 17 isolated clusters were identified, and the localized values of these clusters were filtered from ThunderSTORM's localization data. The center of mass of these clusters was aligned to the origin (0, 0). Then, all such sets were plotted together. The histogram of localizations in the x and y directions was plotted, and the standard deviation from the origin is given as the localization precision in the x and y directions (half of the FWHM). Spot image of isolated clusters was visualized using 20x magnification and the histogram mode of ThunderSTORM.

***C. elegans* culture**

All experiments were performed in *C. elegans* N2 strain obtained from Caenorhabditis Genetics Center (CGC) located in University of Minnesota, USA, funded by National Institutes of Health. The worms were maintained on nematode growth media (NGM) plate, which contains 2% agar (HIMEDIA_GRM026P), 0.25% peptone (HIMEDIA_RM001-500G), 0.3%

NaCl (MERCK_QG4Q641691), 1 mL 1M $CaCl_2$ (LOBA CHEMIE 2466B), 1 mL 1M $MgSO_4$, 25 mL 1 M KPO_4 buffer made from (KH_2PO_4-LOBA CHEMIE 5357B, K_2HPO_4-LOBA CHEMIE 0531), 1 mL 5 mg/mL cholesterol dissolved in ethanol. All the above calculations are done for 1000 mL of solution, which was autoclaved poured into 60 mm plate and solidified before use. Washing of worms during transfer and staining procedures was done using M9 buffer made from 300 mg KH_2PO_4 (LOBA CHEMIE 5357B), 600 mg Na_2HPO_4, 500 mg NaCl (MERCK_QG4Q641691), 0.1 mL $MgSO_4$ mixed in 100 mL distilled water. All buffers and salt solutions are autoclaved before use.

Maintenance

The worms were grown at 20 °C. For feeding 100 µL of *E. coli* OP-50 was added to each NGM plate and then incubated at (25 to 30) ºC for a day, before the worms were added. Worms were transferred from one plate to another by washing a part of the plate with M9 buffer. Depending on the concentration of worms, 50 to 70 µL of M9 was gently poured over a quarter of the plate full of worms. The washed worms from the old plate were collected gently and transferred via pipette onto another the OP-50 seeded NGM plate. For age synchronization, gravid adult *C. elegans* containing NGM plates were washed with 2 mL of M9 buffer, the resultant liquid was collected in a tube and to it was added 4 mL of 4% Sodium Hypochlorite. The solution killed the adults while the eggs within them remained safe. The hypochlorite solution was then removed by washing with M9 buffer via centrifugation at 2000 RPM for 2 minutes twice. The resultant was poured onto empty NGM plates. The emerging worms are now in the same stage because of lack of food, were then collected and transferred onto OP-50 containing plate to grow.

***C. elegans* staining and dissection**

For simple imaging via staining, *C. elegans* were washed out of the NGM plate with M9, then centrifuged at 2000 RPM for 2 minutes while removing supernatant and adding fresh M9 buffer. The procedure was repeated twice to remove residual bacteria, after which they were transferred to a tube containing 2 mL of the buffer. 2 µM of the dye was added to the buffer containing the worms and the resultant was incubated at 20 ºC for 6 h. After this, the worms were again centrifuged twice with M9 as per the protocol above to remove excess stains. After the 2nd step, 10 µL from the resultant pellet was extracted out via pipette and placed on a 2% agar pad so as not to dry out. To immobilize the worms before imaging, 10 µM sodium azide (MERCK-769320) was added to the agar prior to making the pad. A cover slip was added over the pad and the worms were then ready for imaging.

Protocol for staining before dissection used a different technique. 2µM concentration of dye was added along with the OP-50 bacteria to the NGM plate. Worms in L3 to an adult stage were incubated in this plate for 24 h after which they were isolated individually and placed on a slide with a drop of M9. Dissection was done with the help of a 26G syringe needle. A cut was applied to the pharynx or the anus region of the body of the worm after which the embryos were pushed out by the worm's own turgor pressure. The isolated embryos were then collected with the help of a hairbrush and transferred to an agar pad gently via a pipette. A cover slip was attached to the top of the pad before imaging.

Cell culture and staining

HEK and HeLa cells were cultured in Dulbecco's Modified Eagle Medium (DMEM) with 10% fetal bovine serum (FBS). Human monocytic THP-1 cells were maintained in culture in Roswell Park Memorial Institute medium (RPMI) culture medium containing 10% of heat-inactivated fetal bovine serum respectively. THP-1 monocytes are differentiated into macrophages by 24 h incubation with 150 nM phorbol 12-myristate 13-acetate in RPMI media. MDAMB-231 cells were grown in Leibovitz media containing 10% FBS without non-essential amino acid (NEA). The cells were grown with a density of 10^5 cells per well in a live cell culture well. Each well was filled with 2 mL of cell suspension in a growth medium and the cells were allowed to grow overnight for proper adherence and growth. The growth and the attachment of the cells were examined by an optical microscope. Once the cells were properly adhered and confluent, they were stained with Zn-complex around 0.5 h and then brought for imaging.

Confocal imaging

Nikon Eclipse Ti inverted microscope was used for the confocal microscopy and images were acquired using Nikon Nis-Element software. The cell samples were excited by a 488 and 561 nm laser and the emission was collected by using the appropriate filter sets. The colocalization study was performed using a 60x (1.40 NA) oil immersion objective while the mitophagy event was captured by a 100x (1.49 NA) oil immersion objective.

SRRF-Stream

SRRF is an analytical super-resolution microscopy approach where first a stack of images or videos are acquired and then post-processed using NanoJ SRFF plugin of ImageJ developed by the Henriques Lab. SRRF Stream is a highly optimized and advanced version of this algorithm that allows parallel acquisition and recording of super-resolution microscopy data in real-time. SRRF stream software operates on the micro-manager of ImageJ and was purchased from Andor.

SRRF-Stream imaging was performed using an Andor iXon Ultra 897U EMCCD camera and a Nikon Eclipse Ti inverted microscope. The sample was illuminated by a lamp using an excitation filter of 540/25 nm and the emission was collected by a 605/55 nm filter. A 565 nm dichroic (RDC) mirror was used to separate the excitation light and emission observed from the sample. Images were obtained with a Nikon 100x 1.45 NA Plan Apo oil immersion objective. The CCD chip was cooled to -80 °C to decrease dark counts related to image noise. Using a micro-manager software package in ImageJ, videos were recorded with SRRF enabled. 100 frames with 20 ms exposure time were taken to create one frame of super-resolution video. Pre amp Gain-3, Pixel readout rate-17 MHz, EM Gain (adjustable from 50 to 300), radiality magnification-5, and ring radius-1 were used for data acquisition.

Distance and speed mapping

Distance-calibrated super-resolution videos showing lysosomal motion were obtained via SRRF-stream as discussed in the above section. A macro language script for ImageJ (Fiji) was made, enabling users to manually track each lysosome. The script records the x and y coordinates for each lysosome in a single cell across 50 frames. Additionally, it computes the total distance travelled, average speed, as well as speed and distance per frame. The process was repeated for perinuclear and peripheral regions of various cells. Data was compiled and plotted using origin.

Cell viability

For cell viability assessment, HeLa cells were seeded in 96 well plates at a density of 5000 cells per well. After overnight incubation, the cells were washed with 1X PBS, and the media was replaced with fresh DMEM and Zn-complex. After 6, 12, and 24 h of incubation, 40 µL of XTT labeling mixture: 5 mL XTT labeling reagent with 0.1 mL electron coupling reagent (Cell proliferation Kit II-XTT Roche) was added to each well and further incubated for 12 h. Tetrazolium salt XTT was cleaved in the presence of an electron-coupling reagent to produce soluble formazan salts, and the absorbance was read at 570 nm with a reference read at 650 nm using a Tecan Infinite M200 PRO plate reader.

Synthesis and Characterization

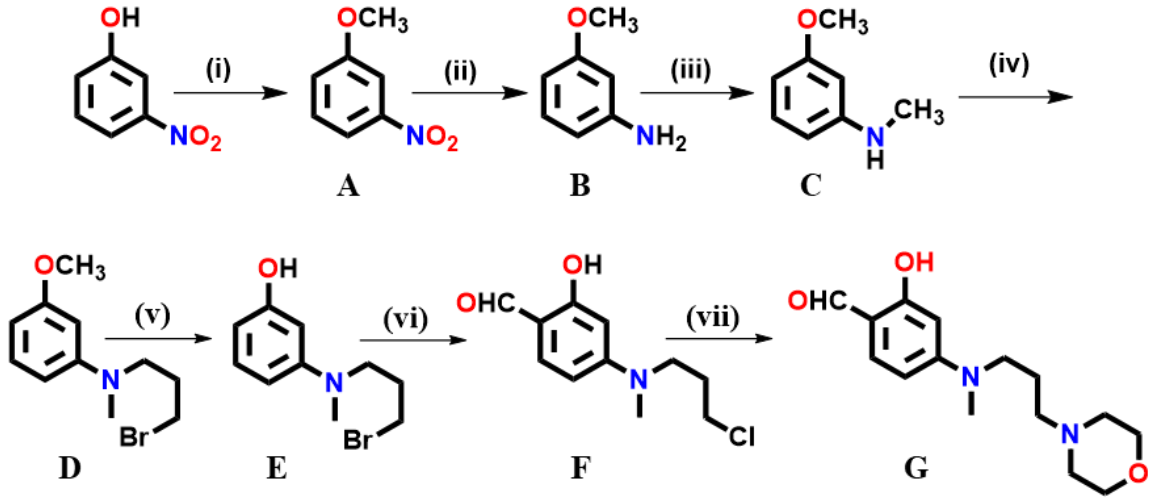

(i) K_2CO_3, DMF, MeI, 5 h RT (ii) $SnCl_2$, HCl, EtOH, 6h reflux; (iii) (a) $(CH_2O)n$, NaOMe, 16 h; (b) $NaBH_4$, 3 h reflux. (iv) 1,3-dibromopropane, $KHCO_3$, ACN, 12 h at RT; (v) BBr_3, DCM, 0 °C; (vi) $POCl_3$, DMF; (vii) K_2CO_3, morpholine at RT (viii) Ethanol, 85 °C, 16 h.

Scheme S1: Synthetic route for the formation of compound G.

Compound A: 3-nitro anisole: To a solution of 3-nitrophenol (3 gm, 21.56 mmoles), and potassium carbonate (5.96 gm, 43.13 mmoles) in 40 mL dimethylformamide, Me-I (43.13 mmoles, 6.102 gm) was added slowly, and the mixture was stirred at ambient temperature for 12 h. After 12 h, the reaction mixture was extracted with ethyl acetate and dried using sodium sulphate (yield: 3.68 gm). **^{1}H-NMR (500 MHz $CDCl_3$-d:)** δ 7.78 (dd, J = 8.3, 2.5 Hz, 1H), 7.68 (t, J = 2.4 Hz, 1H), 7.40 (t, J = 8.2 Hz, 1H), 7.19 (dd, J = 8.3, 2.7 Hz, 1H), 3.86 (s, 3H).

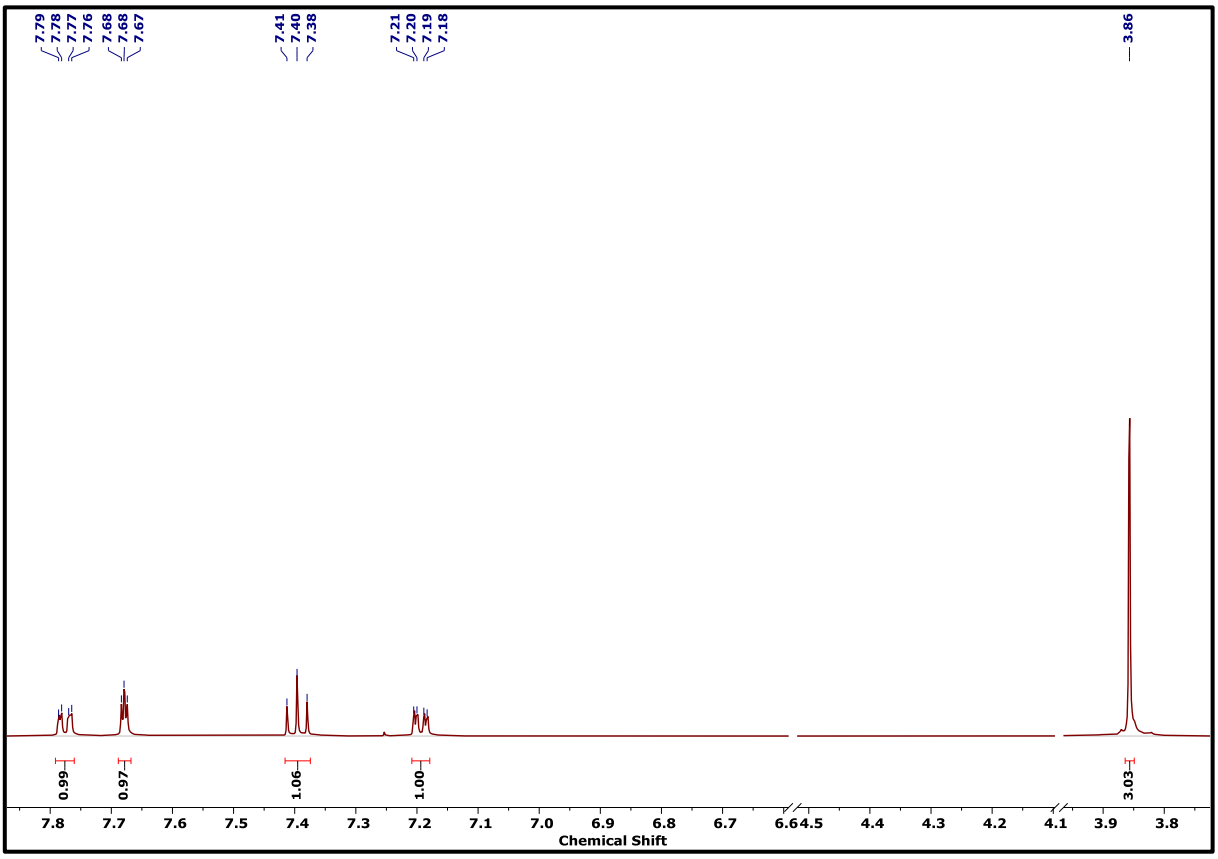

Fig. S1: ^{1}H-NMR spectra of compound A.

Compound B: 3-amino anisole: A mixture of 3-nitro anisole (1.1 gm, 7.2 mmoles), anhydrous $SnCl_2$ (6.5 gm, 28.73 mmoles), was dissolved in HCl/ethanol of 1:1 ratio, and the resulting solution was allowed to reflux for 6 h under a nitrogen atmosphere. After the reaction, the solution was neutralized using sodium hydroxide in an ice bath and was filtered through a Buchner funnel. The obtained mixture was extracted with ethyl acetate and purified by column chromatography to give dark yellow oil (yield: 0.65 gm). **^{1}H-NMR (500 MHz $CDCl_3$-d):** δ 7.07 (t, *J* = 7.9 Hz, 1H), 6.32 (m, *J* = 16.9, 8.2, 2.5 Hz, 2H), 6.25 (t, *J* = 2.3 Hz, 1H), 3.77 (s, 3H), 3.67 (s, 2H).

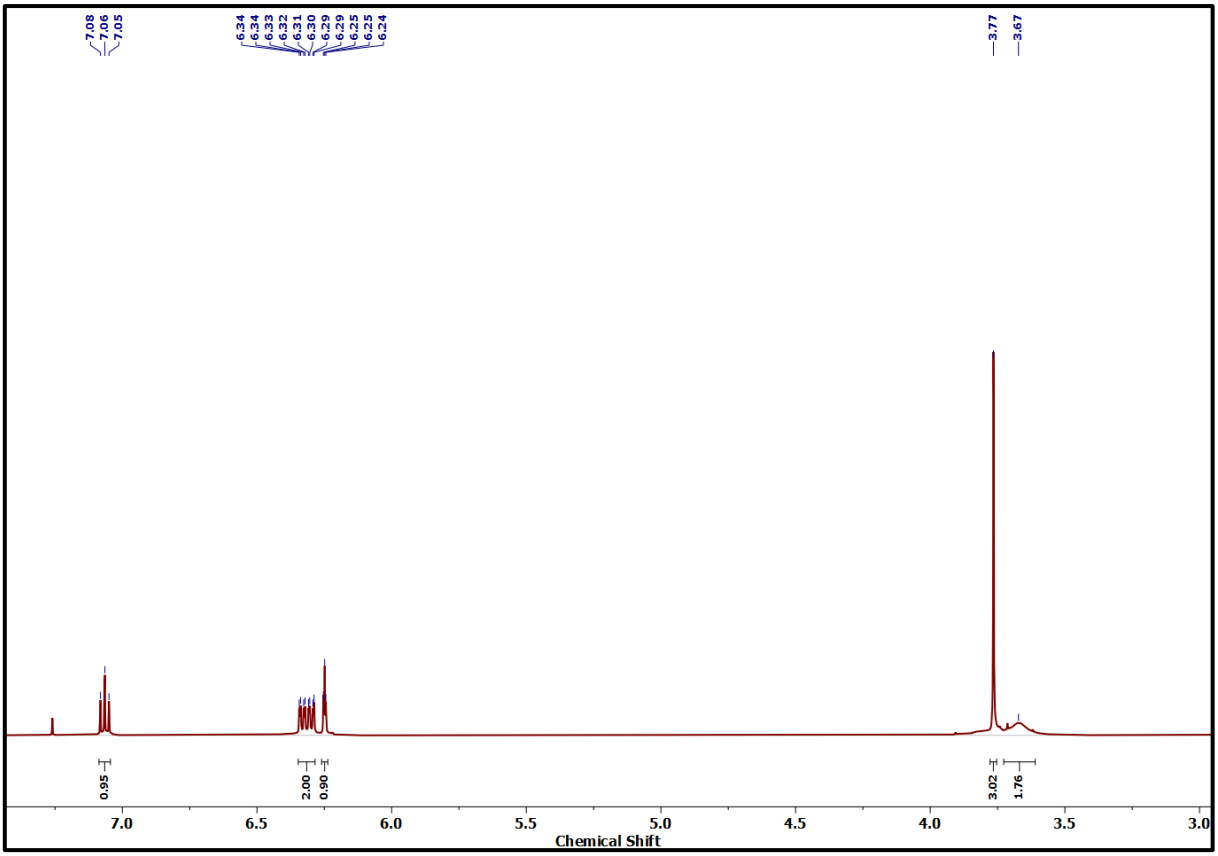

Fig. S2: ^{1}H-NMR spectra of compound B.

Compound C: 3-methoxy-N-methylaniline: To a solution of 3-amino anisole (3.28 gm, 26.7 mmoles) and sodium methoxide (7.02 gm, 133 mmoles) in methanol, paraformaldehyde (1.60 gm, 53.30 mmoles) was added slowly, and the reaction mixture was stirred at room temperature for 16 h. Then sodium borohydride (1.01 gm, 26.70 mmoles) was added to the reaction mixture. After refluxing for 2 h, the mixture was concentrated by evaporating the solvent, treated with 1 M KOH, and then extracted with ethyl acetate. The combined organic layer was dried over Na_2SO_4 and evaporated to give the crude product. The obtained product was purified by silica gel column chromatography to provide a pure product as a yellow oil (yield: 3.0 gm). **^{1}H NMR (500 MHz, $CDCl_3$-d):** δ 7.18 (t, *J* = 8.1 Hz, 1H), 6.42 – 6.36 (m, 1H), 6.32 (d, *J* = 8.2 Hz, 2H), 3.83 (s, 3H), 3.49 (dt, *J* = 16.0, 6.5 Hz, 4H), 2.98 (s, 3H), 2.16 (p, *J* = 6.4 Hz, 2H).

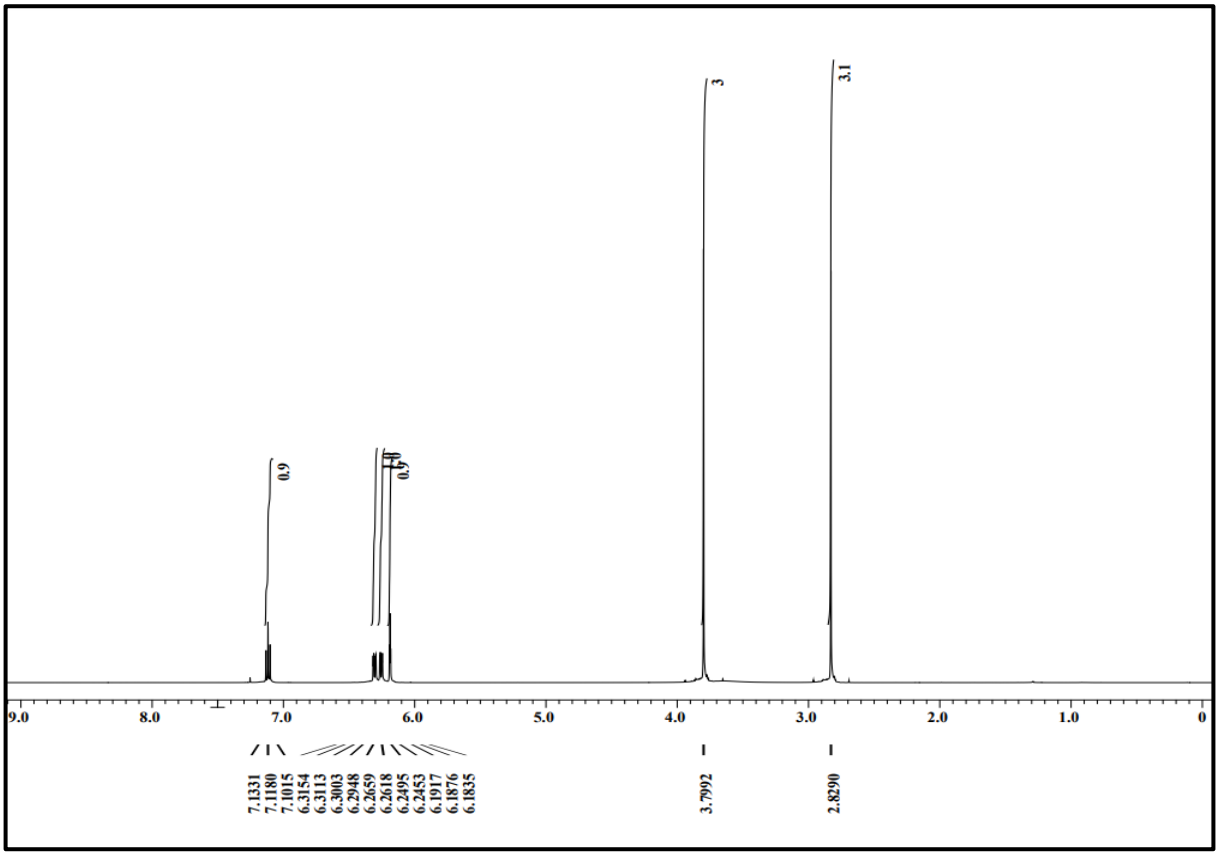

Fig. S3: ^{1}H-NMR spectra of compound C.

Compound D: N-(3-bromopropyl)-3-methoxy-N-methylaniline: A mixture of (2.0 gm, 14.6 mmoles) of 3-methoxy-N-methylaniline, (15 gm ,74.2 mmoles) of 1,3-dibromopropane and (1.54 gm, 15.3 mmoles) of $KHCO_3$ were dissolved in 30 mL of CH_3CN, and the solution was refluxed under inert atmosphere for 6 h. After the reaction, the solvent was removed under the reduced pressure. The brown residue was extracted with CH_2Cl_2 and then purified by column chromatography to give yellow oil (yield: 2 gm). **^{1}H NMR (500 MHz, $CDCl_3$-d):** δ 7.18 (t, J = 8.1 Hz, 1H), 6.41 – 6.37 (m, 1H), 6.32 (d, J = 8.2 Hz, 2H), 3.83 (s, 3H), 3.49 (dt, J = 16.0, 6.5 Hz, 4H), 2.98 (s, 3H), 2.16 (m, 2H).

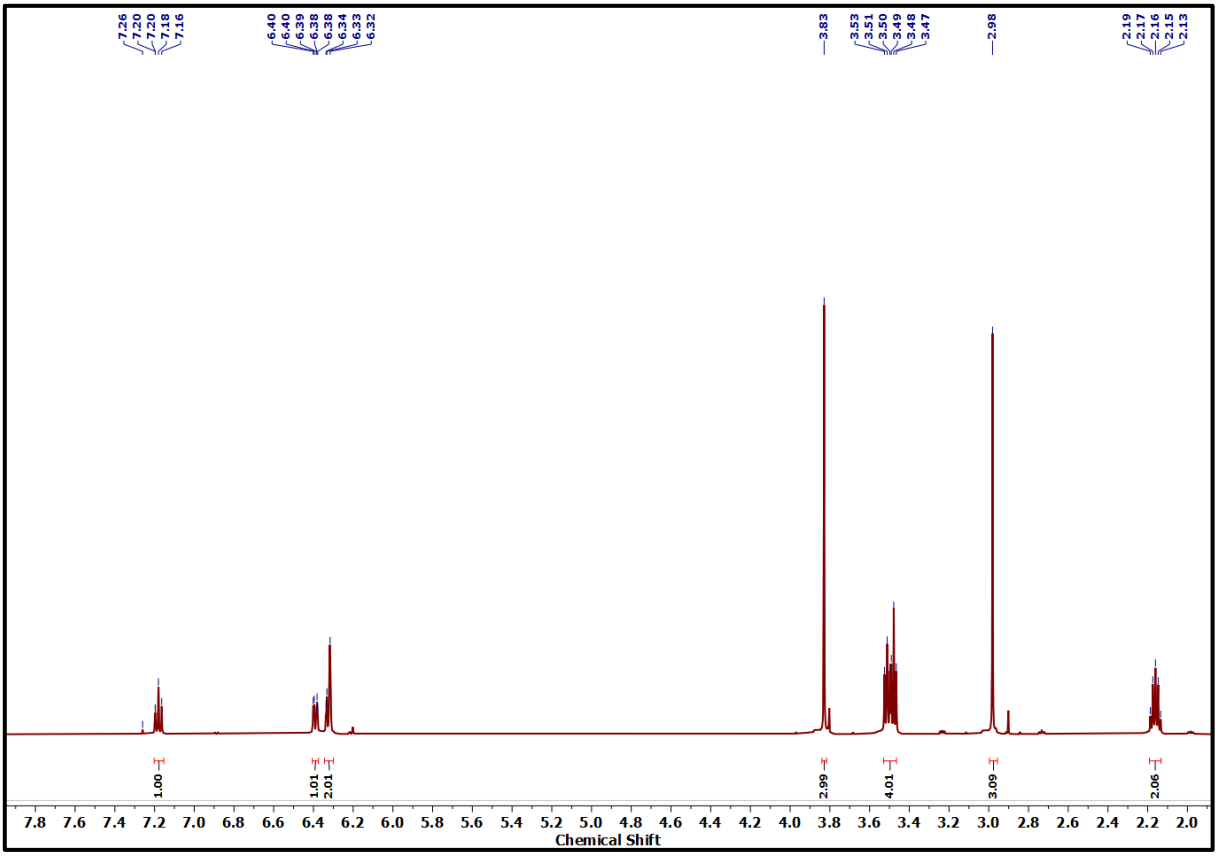

Fig. S4: ^{1}H-NMR spectra of compound D.

Compound E: 3-((3-bromopropyl)(methyl)amino)phenol: Compound D (2.10 gm, 8.1 mmoles) was dissolved in 15 mL of dichloromethane. BBr_3 (1.0 mL, 10.6 mmoles) was added to the solution at 0 °C in an ice bath, and the solution was slowly warmed to room temperature and stirred overnight. Added iced methanol to the solution in an ice bath, and the solvent was removed under reduced pressure. Then, the product was purified by column chromatography to give light yellow oil (yield: 1.06 gm). **^{1}H NMR (500 MHz, $CDCl_3$-*d*):** δ 7.10 (t, *J* = 8.2 Hz, 1H), 6.40 – 6.32 (m, 2H), 6.27 (d, *J* = 7.9 Hz, 1H), 3.46 (m, *J* = 18.5, 6.6 Hz, 4H), 2.96 (s, 3H), 2.18 – 2.08 (m, 2H).

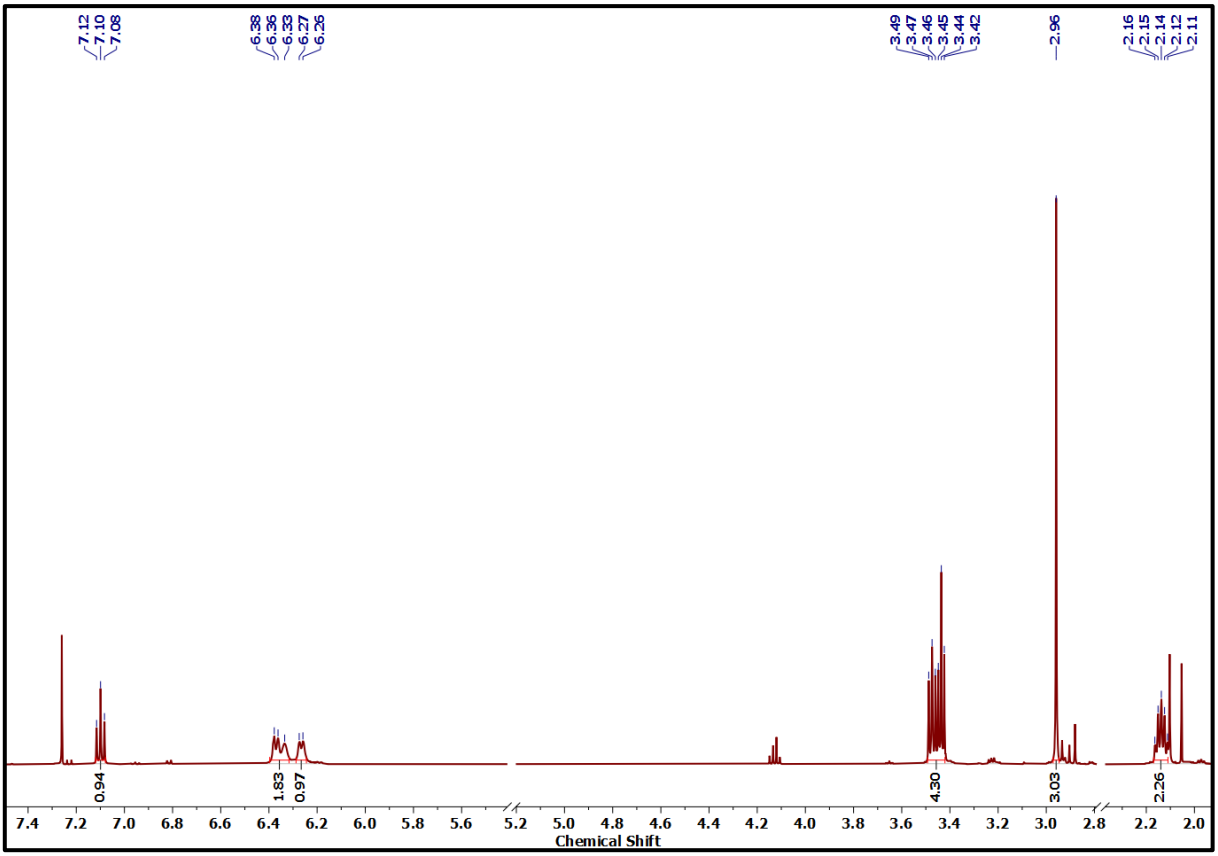

Fig. S5: ^{1}H-NMR spectra compound E.

Compound F: 4-((3-chloropropyl)(methyl)amino)-2-hydroxybenzaldehyde: $POCl_3$ (0.9 mL) was added slowly in dry DMF at 0 °C and stirred for 30 minutes. Then compound E (1.01 gm, 4.1 mmoles) in dry DMF was added slowly to the reaction mixture at 0 °C. The solution was gradually warmed to room temperature and agitated for 12 h. Then, the reaction mixture was dropped into ice and stirred for 10-15 minutes. The product was extracted with DCM and then purified using column chromatography to produce pure product as a yellow oil (yield: 0.75 gm). **^{1}H NMR (500 MHz, $CDCl_3$-*d*)**: δ 11.59 (s, 1H), 9.53 (s, 1H), 7.30 (d, *J* = 8.3 Hz, 1H), 6.32 (dd, *J* = 8.6, 2.4 Hz, 1H), 6.10 (d, *J* = 2.2 Hz, 1H), 3.59 (m, *J* = 8.9, 5.8, 3.1 Hz, 4H), 3.07 (s, 3H), 2.21 – 2.08 (m, 2H).

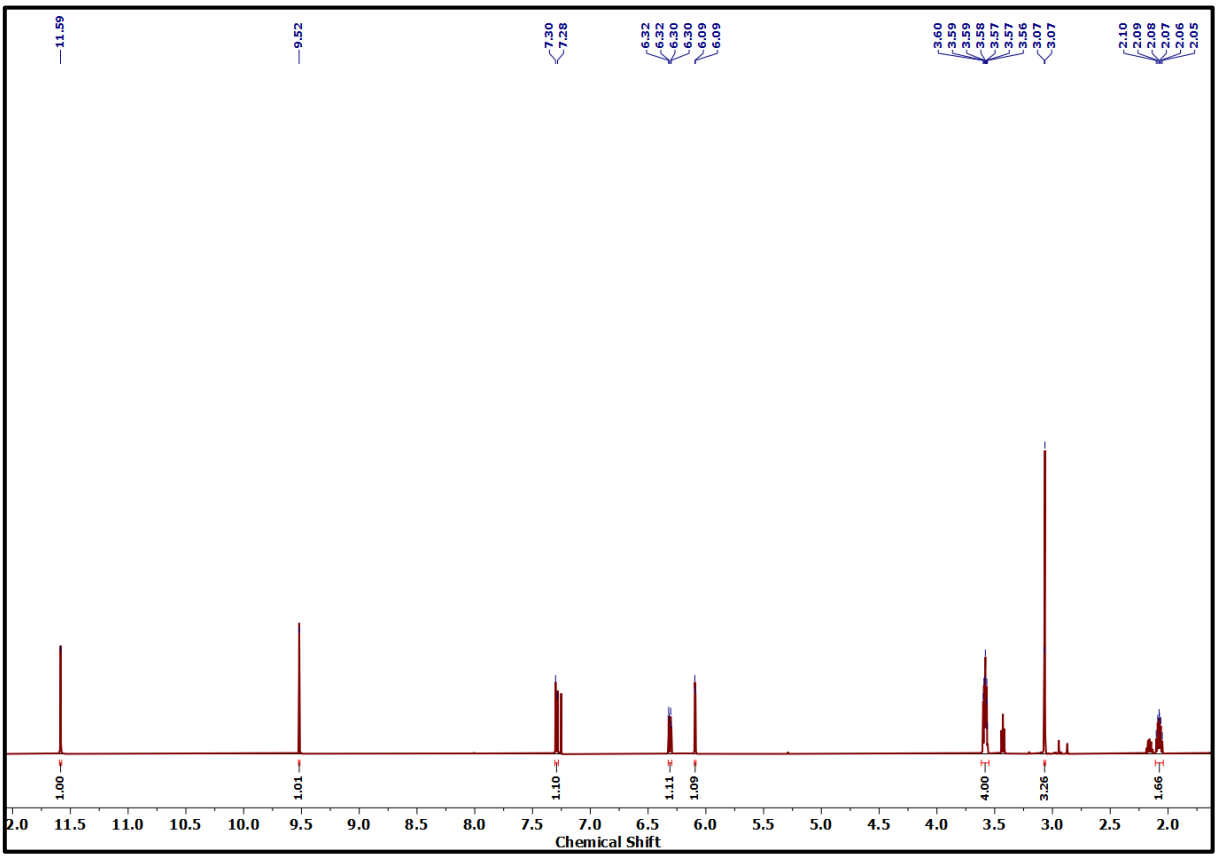

Fig. S6: ^{1}H-NMR spectra compound F.

Compound G. 2-hydroxy-4-(methyl(3-morpholinopropyl)amino)benzaldehyde: A mixture of compound F (150 mg, 0.66 mmoles), $KHCO_3$, (66 mg, 0.66 mmoles) and morpholine (490 mg, 5.62 mmoles) were dissolved in 30 mL of CH_3CN, the solution was refluxed under nitrogen overnight, and the solvent was removed under the reduced pressure. The brown residue was extracted with CH_2Cl_2 and then purified by column chromatography to give yellow oil (yield: 80 mg). **^{1}H NMR (500 MHz, $CDCl_3$-*d*):** δ 11.59 (s, 1H), 9.51 (s, 1H), 7.28 (s, 0H), 6.32 (dd, J = 8.9, 2.6 Hz, 1H), 6.14 (d, J = 2.6 Hz, 1H), 3.74 (t, J = 4.5 Hz, 4H), 3.47 (t, J = 7.1 Hz, 2H), 3.04 (s, 2H), 2.44 (s, 4H), 2.35 (t, J = 6.9 Hz, 2H), 1.79 (m, 2H).

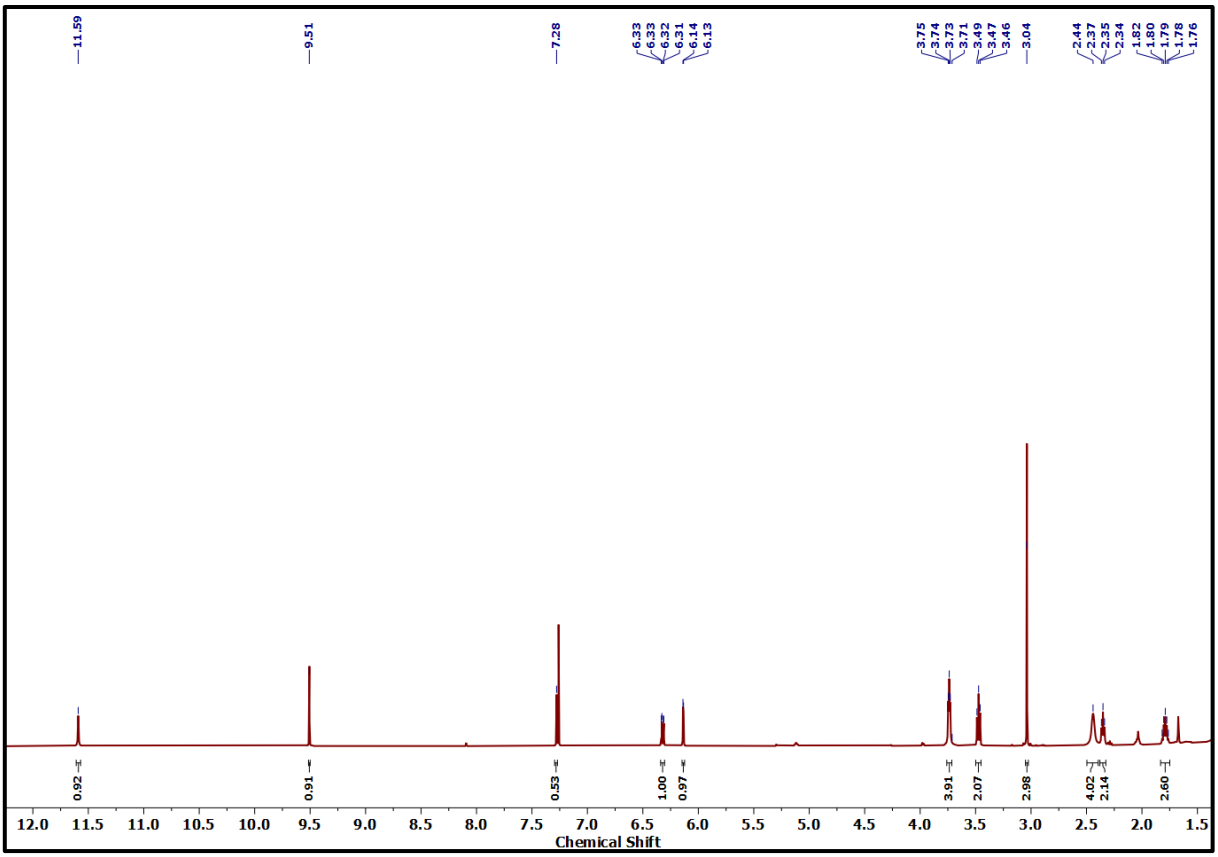

Fig. S7: ^{1}H-NMR spectra compound G.

Zn-complex: A mixture of compound G (45 mg, 0.16 mmoles), diaminomaleonitrile (8.74 mg, 0.081 mmoles), and of $Zn(OAc)_2 \cdot 2H_2O$ (17.75 mg, 0.81 mmoles) was dissolved in 2-3 mL of ethanol and refluxed overnight. The solvent was removed in vacuo, and the crude product was washed repeatedly with iced ethanol to give dark green solid as Zn-complex (yield: 30 mg). **^{1}H NMR (500 MHz, DMSO-d_6):** δ 8.10 (s, 1H), 7.12 (d, J = 9.1 Hz, 1H), 6.27 (dd, J = 9.4, 2.6 Hz, 1H), 5.81 (d, J = 2.5 Hz, 1H), 3.55 (d, J = 4.7 Hz, 3H), 3.41 (t, J = 7.1 Hz, 2H), 2.98 (s, 2H), 2.33 – 2.30 (m, 3H), 2.27 (t, J = 6.9 Hz, 1H), 1.68 (m, 2H).

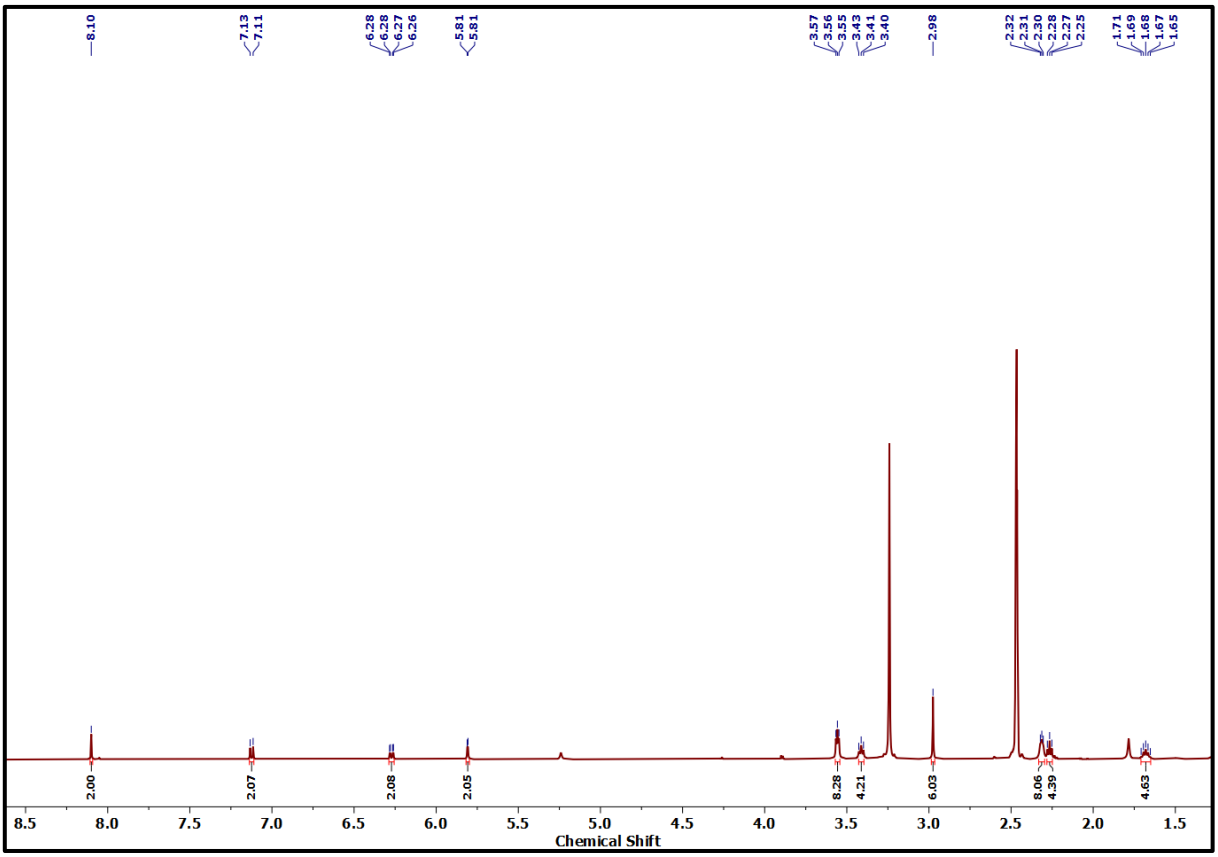

Fig. S8: ^{1}H-NMR spectra compound Zn-complex.

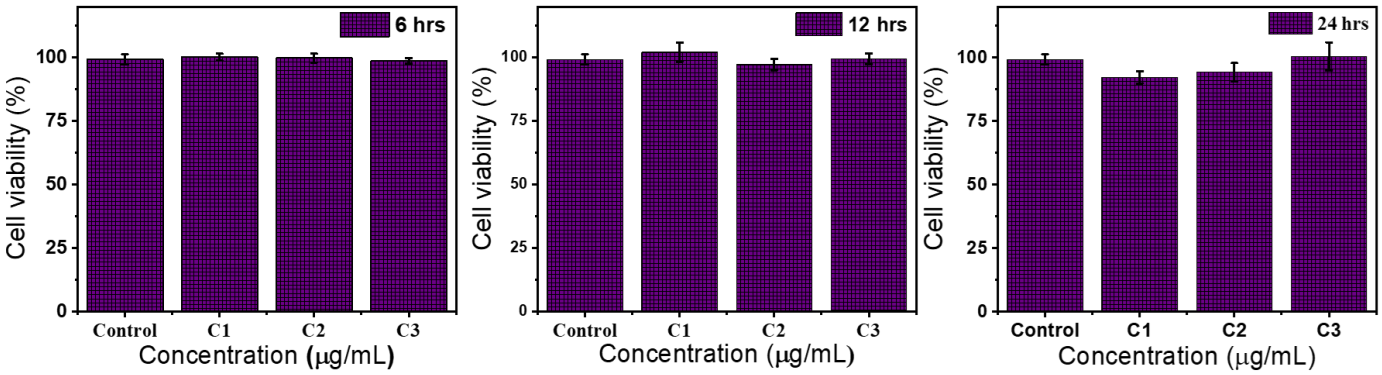

Fig. S9: Cell viability of HeLa cells after treatment of Zn-complex: (a) 6 h, (b) 12 h, and (c) 24 h duration time with control at three different concentrations as C1= 0.70 μg/mL, C2 = 1.38 μg/mL, C3 = 2.76 μg/mL, respectively. The cell viability data shows the non-toxic nature of Zn-complex.

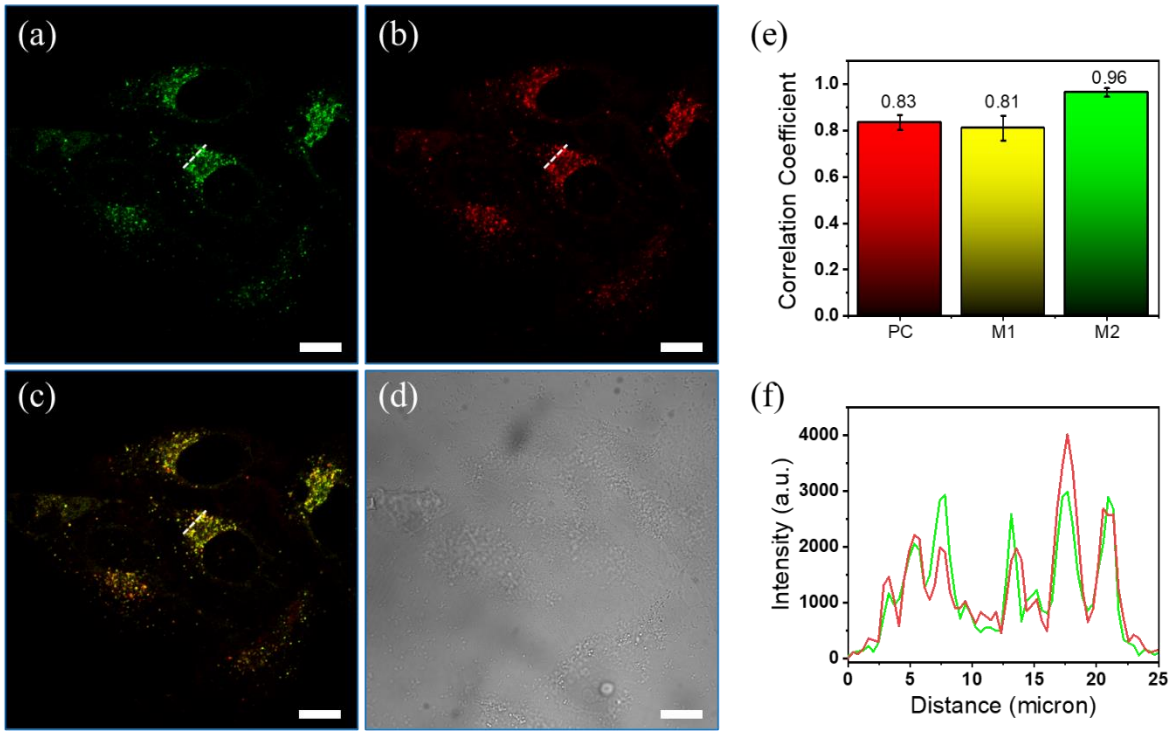

Fig. S10: Subcellular co-localization of HeLa cells stained with Zn-complex and LTG: (a) Represent the lysosomes stained with LTG visualized in 500-550 nm range (green channel). (b) Represent the lysosomes stained with Zn-complex visualized in 570-620 nm range (red channel). (c) overlay panel of (a) and (b). (d) Transmission detection image. (e) The degree of colocalization between the LTG (Green) and Zn-complex (red) panels and is expressed with Pearson's correlation coefficient (PCC) and Mander's colocalization coefficients M1 and M2. (f) The Intensity profile along the drawn white line in confocal images. Scale bar: 10 μm

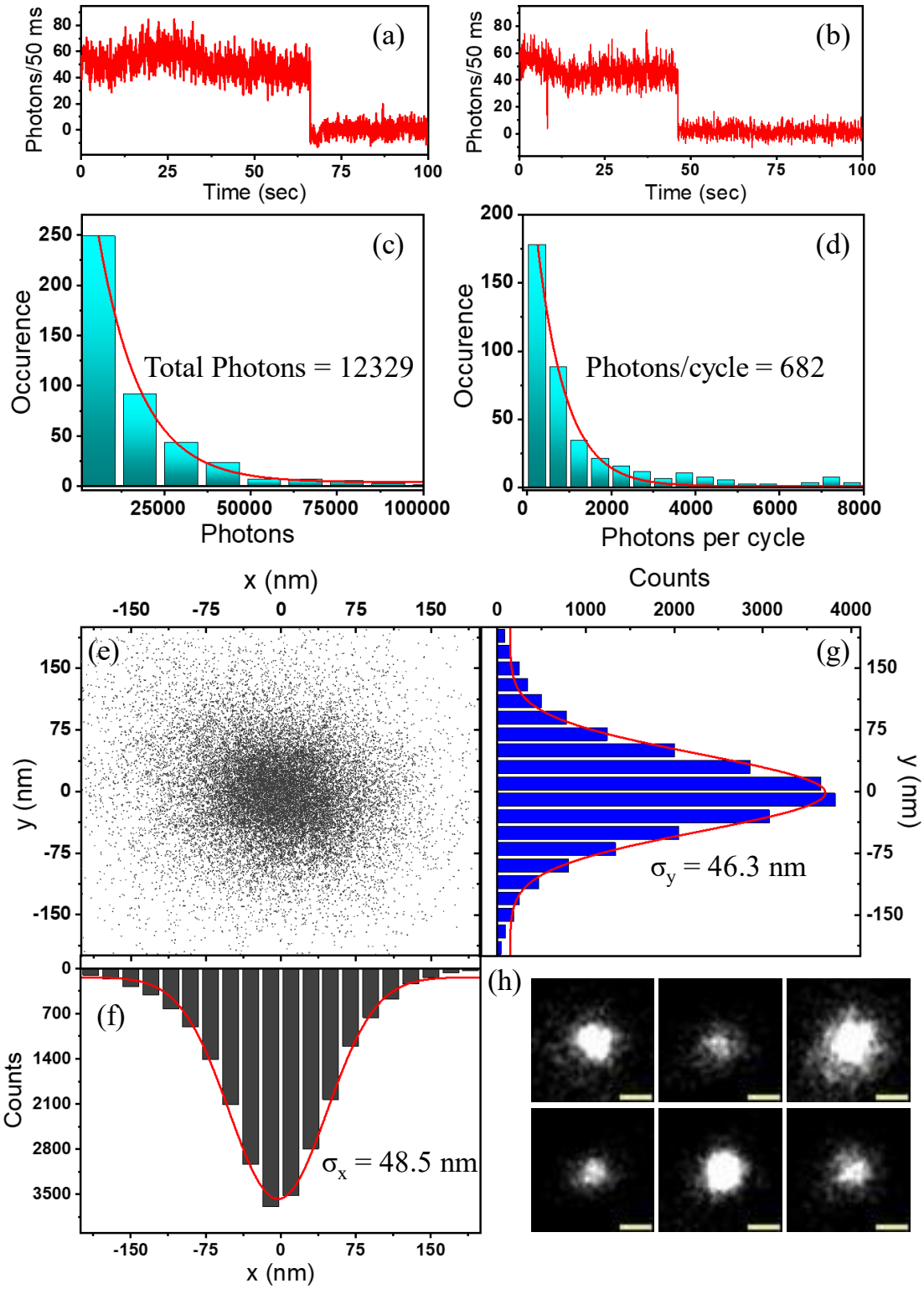

Fig. S11: Single-molecule fluorescence spectroscopy of Zn-complex: (a, b) Single-molecule time traces of the Zn-complex showing single-step bleaching, (c) Total photon counts, (d) Photons per cycle, and (e) Scattered plot formed by aligning the center of mass of 10-15 spot's localisations at origin. (f and g) show the average localization precision for a single Zn-complex spot obtained as ~48.5 nm in the x direction and ~46.3 nm in the y-direction. (h) Localized reconstruction image of a single Zn-complex spot. Scale bar: 100 nm

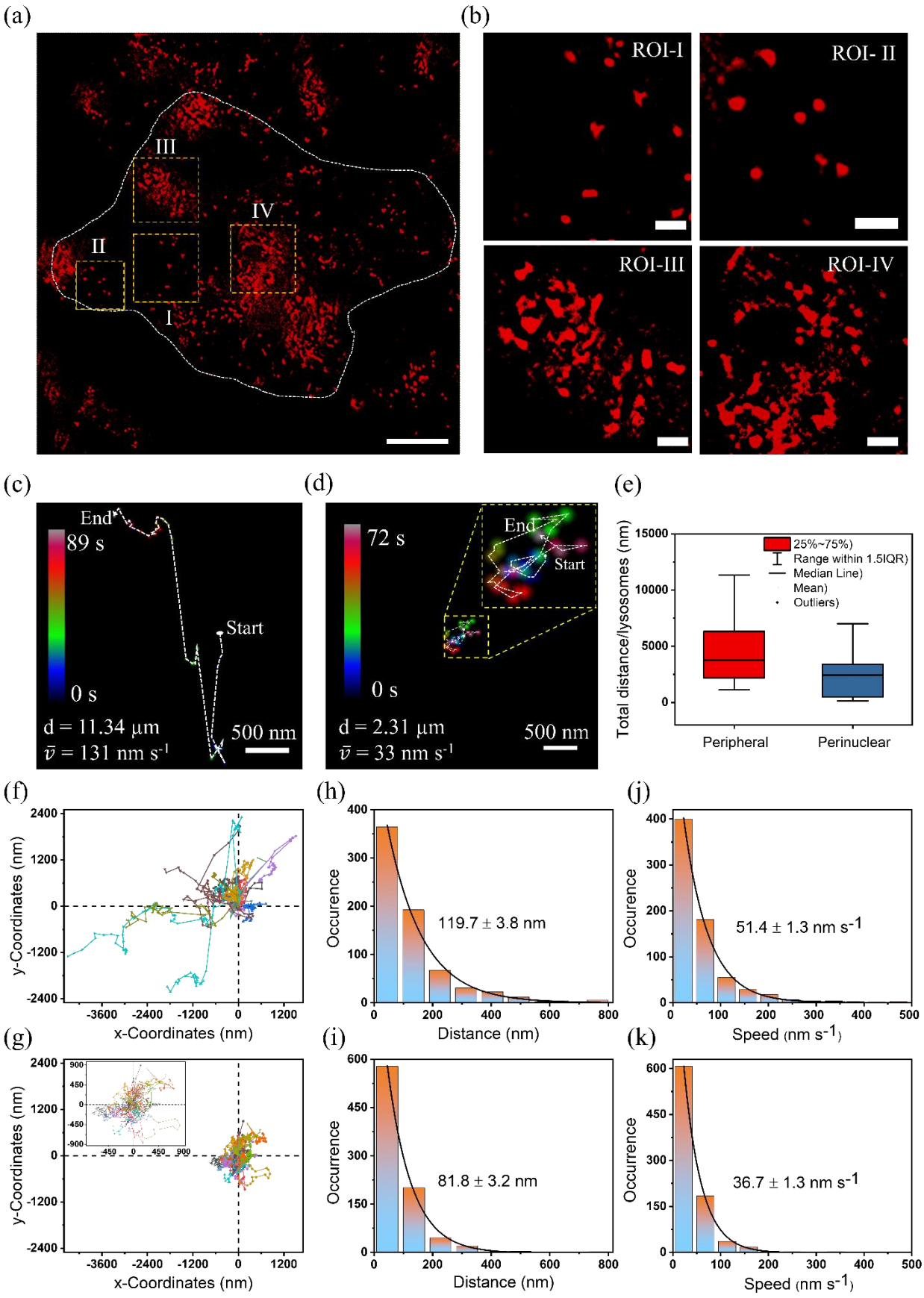
(a)
III
IV
II
I
(b)
ROI-I
ROI- II
ROI-III
ROI-IV
(c)
End
89 s
Start
0 s
d = 11.34 μm
$\bar{v}$ = 131 nm s^{-1}
500 nm
(d)
72 s
End
Start
0 s
d = 2.31 μm
$\bar{v}$ = 33 nm s^{-1}
500 nm
(e)
Total distance/lysosomes (nm)
25%~75%)
Range within 1.5IQR)
Median Line)
Mean)
Outliers)
Peripheral
Perinuclear
(f)
y-Coordinates (nm)
x-Coordinates (nm)
(g)
y-Coordinates (nm)
x-Coordinates (nm)
(h)
Occurence
119.7 ± 3.8 nm
Distance (nm)
(i)
Occurence
81.8 ± 3.2 nm
Distance (nm)
(j)
Occurence
51.4 ± 1.3 nm s^{-1}
Speed (nm s^{-1})
(k)
Occurence
36.7 ± 1.3 nm s^{-1}
Speed (nm s^{-1})

Fig. S12: Live-cell lysosomal tracking utilizing super-resolution microscopy in HEK cells: (a) SRRF imaging of whole cells displaying lysosomes labeled with the Zn-complex in live HEK cells. Scale bar: 10 μm. (b) SRRF imaging focusing on peripheral lysosomes (ROI-1, ROI-II) and perinuclear lysosomes (ROI-III, ROI-IV). Scale bar: 1 μm. (c, d) Representative trajectories of individual lysosome movement displayed by a white dot (indicating the starting point) and a white arrowhead (indicating the end position) for peripheral and perinuclear regions, respectively. (e) Box plot illustrating the total distance traveled per lysosome over 50 frames (~108 s). (f) Trajectories of approximately 25 individual lysosomes, originating from the origin in the peripheral region. (g) Trajectories of lysosomes starting from the origin in the perinuclear region. (h) Histogram presenting the distance traveled by all lysosomes within a single frame in the peripheral region, showing an average value of 119.7 nm. (i) Histogram displaying the distance traveled by lysosomes in the perinuclear region within a single frame, with an average value of 81.8 nm. (j) Histogram showcasing the speeds of all lysosomes in a single frame for the peripheral region, demonstrating an average value of 51.4 nm s^{-1}. (k) Histogram illustrating the speeds of lysosomes in the perinuclear region within a single frame, averaging at 36.7 nm s^{-1}.

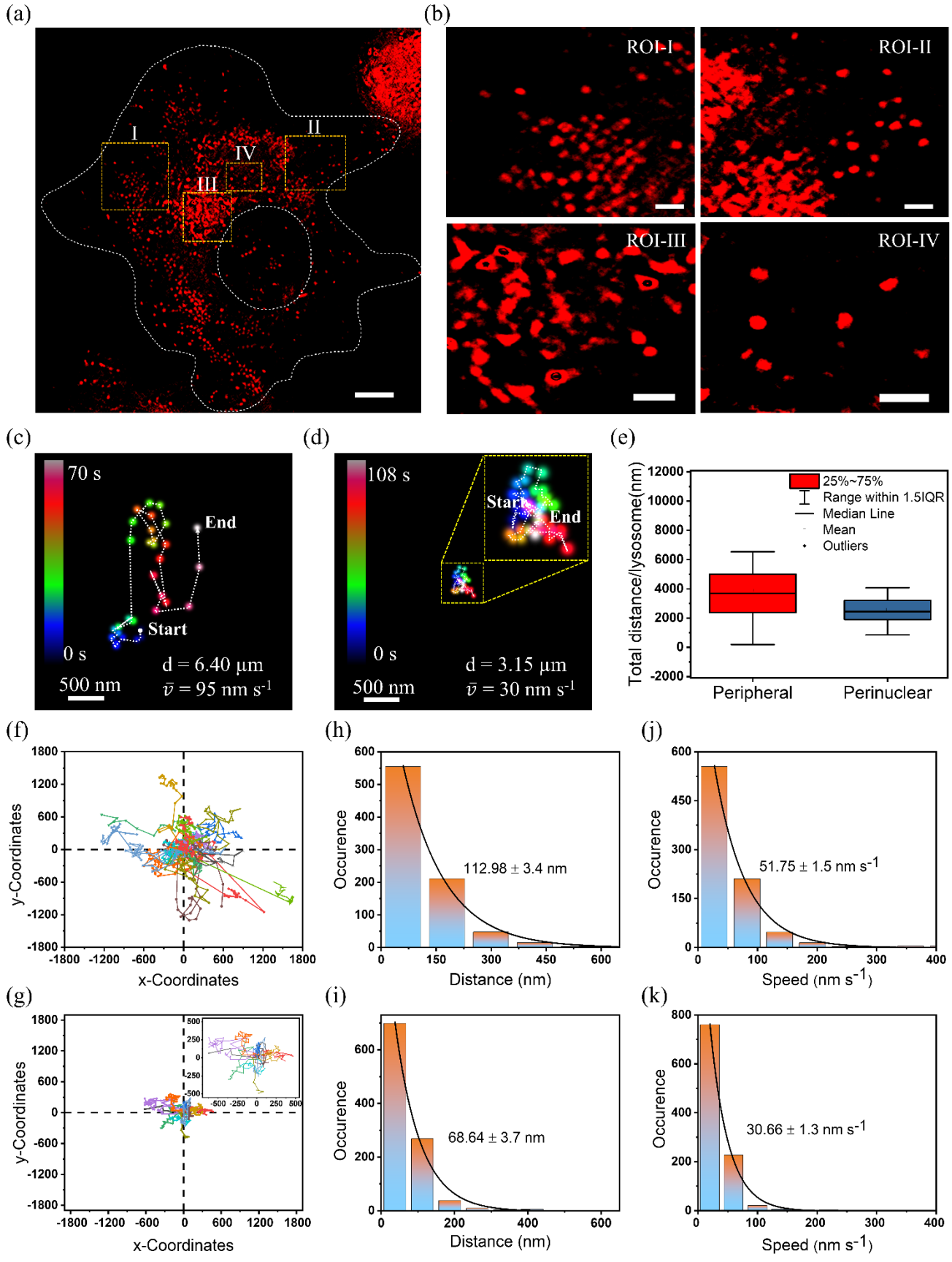
(a)
I
II
III
IV
(b)
ROI-I
ROI-II
ROI-III
ROI-IV
(c)
70 s
End
Start
0 s
d = 6.40 μm
$\bar{v}$ = 95 nm s^{-1}
500 nm
(d)
108 s
Start
End
0 s
d = 3.15 μm
$\bar{v}$ = 30 nm s^{-1}
500 nm
(e)
Total distance/lysosome(nm)
25%~75%
Range within 1.5IQR
Median Line
Mean
Outliers
Peripheral
Perinuclear
(f)
y-Coordinates
x-Coordinates
(g)
y-Coordinates
x-Coordinates
(h)
Occurence
112.98 ± 3.4 nm
Distance (nm)
(i)
Occurence
68.64 ± 3.7 nm
Distance (nm)
(j)
Occurence
51.75 ± 1.5 nm s^{-1}
Speed (nm s^{-1})
(k)
Occurence
30.66 ± 1.3 nm s^{-1}
Speed (nm s^{-1})

Fig. S13: Live-cell lysosomal tracking utilizing super-resolution microscopy in THP-1 cells: (a) Long-term SRRF imaging of whole cells displaying lysosomes labeled with the Zn-complex in live THP-1 cells. Scale bar: 5 μm. (b) SRRF imaging focusing on peripheral lysosomes (ROI-1, ROI-II) and perinuclear lysosomes (ROI-III, ROI-IV). Scale bar: 0.5 μm. (c, d) Representative trajectories of individual lysosome movement displayed by a white dot (indicating the starting point) and a white arrowhead (indicating the end position) for peripheral and perinuclear regions, respectively. (e) Box plot illustrating the total distance traveled per lysosome over 50 frames (~108 s). (f) Trajectories of approximately 25 individual lysosomes, originating from the origin in the peripheral region. (g) Trajectories of lysosomes starting from the origin in the perinuclear region. (h) Histogram presenting the distance traveled by all lysosomes within a single frame in the peripheral region, showing an average value of 112.98 nm. (i) Histogram displaying the distance traveled by lysosomes in the perinuclear region within a single frame, with an average value of 68.64 nm. (j) Histogram showcasing the speeds of all lysosomes in a single frame for the peripheral region, demonstrating an average value of 51.75 nm s^{-1}. (k) Histogram illustrating the speeds of lysosomes in the perinuclear region within a single frame, averaging at 30.66 nm s^{-1}.

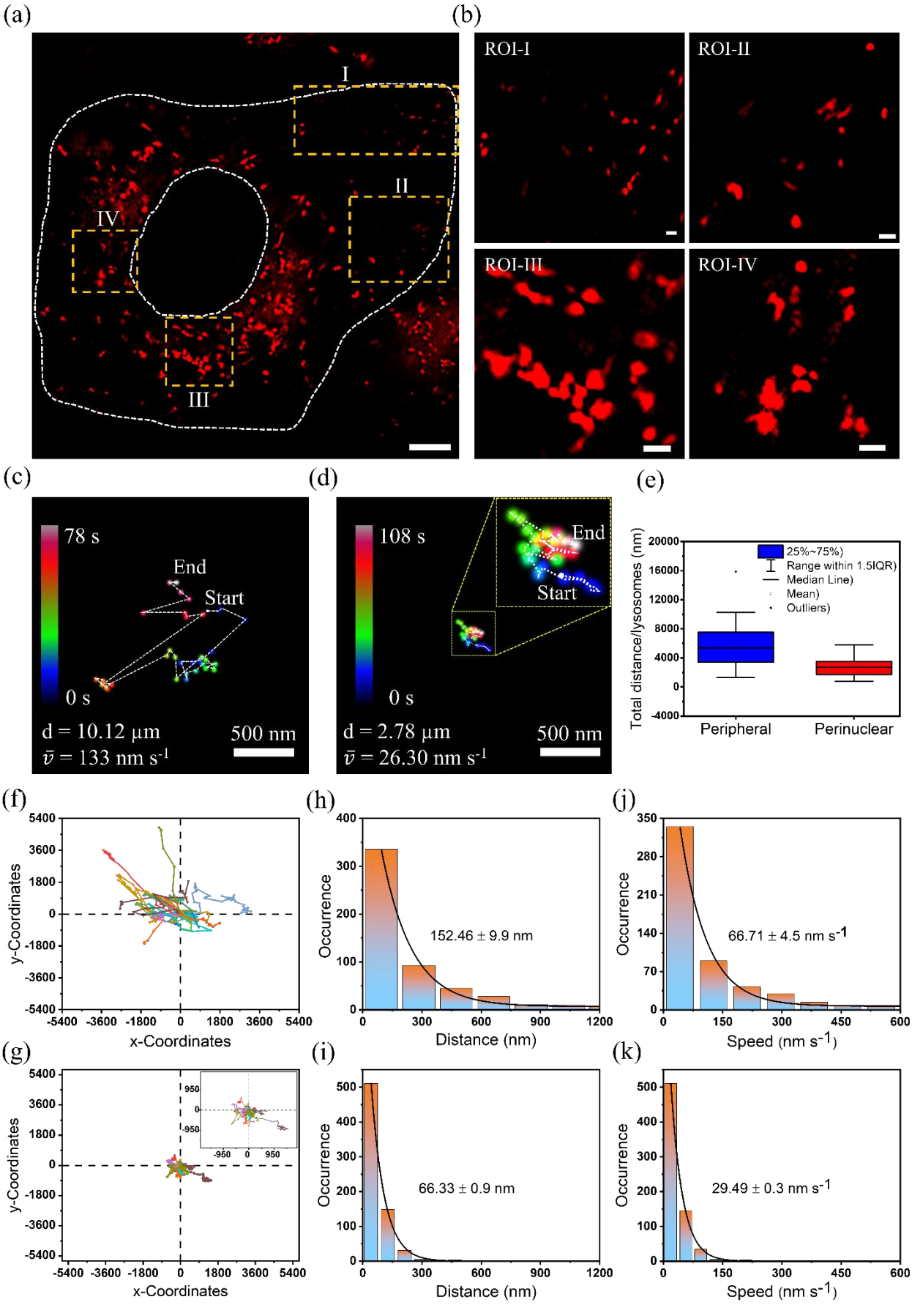
(a)
I
II
III
IV
(b)
ROI-I
ROI-II
ROI-III
ROI-IV
(c)
78 s
0 s
End
Start
d = 10.12 μm
$\bar{v}$ = 133 nm s^{-1}
500 nm
(d)
108 s
0 s
End
Start
d = 2.78 μm
$\bar{v}$ = 26.30 nm s^{-1}
500 nm
(e)
Total distance/lysosomes (nm)
25%~75%)
Range within 1.5IQR)
Median Line)
Mean)
Outliers)
Peripheral
Perinuclear
(f)
y-Coordinates
x-Coordinates
(g)
y-Coordinates
x-Coordinates
(h)
Occurrence
152.46 ± 9.9 nm
Distance (nm)
(i)
Occurrence
66.33 ± 0.9 nm
Distance (nm)
(j)
Occurrence
66.71 ± 4.5 nm s^{-1}
Speed (nm s^{-1})
(k)
Occurrence
29.49 ± 0.3 nm s^{-1}
Speed (nm s^{-1})

Fig. S14: Live-cell lysosomal tracking utilizing super-resolution microscopy in MDA-MB-231 cells: (a) Long-term SRRF imaging of whole cells displaying lysosomes labeled with the Zn-complex in live MDA-MB-231 cells. Scale bar: 5 µm. (b) SRRF imaging focusing on peripheral lysosomes (ROI-1, ROI-II) and perinuclear lysosomes (ROI-III, ROI-IV). Scale bar: 0.5 µm. (c, d) Representative trajectories of individual lysosome movement displayed by a white dot (indicating the starting point) and a white arrowhead (indicating the end position) for peripheral and perinuclear regions, respectively. (e) Box plot illustrating the total distance traveled per lysosome over 50 frames (~108 s). (f) Trajectories of approximately 25 individual lysosomes, originating from the origin in the peripheral region. (g) Trajectories of lysosomes starting from the origin in the perinuclear region. (h) Histogram presenting the distance traveled by all lysosomes within a single frame in the peripheral region, showing an average value of 152.46 nm. (i) Histogram displaying the distance traveled by lysosomes in the perinuclear region within a single frame, with an average value of 66.33 nm. (j) Histogram showcasing the speeds of all lysosomes in a single frame for the peripheral region, demonstrating an average value of 66.71 nm s^{-1}. (k) Histogram illustrating the speeds of lysosomes in the perinuclear region within a single frame, averaging at 24.49 nm s^{-1}.

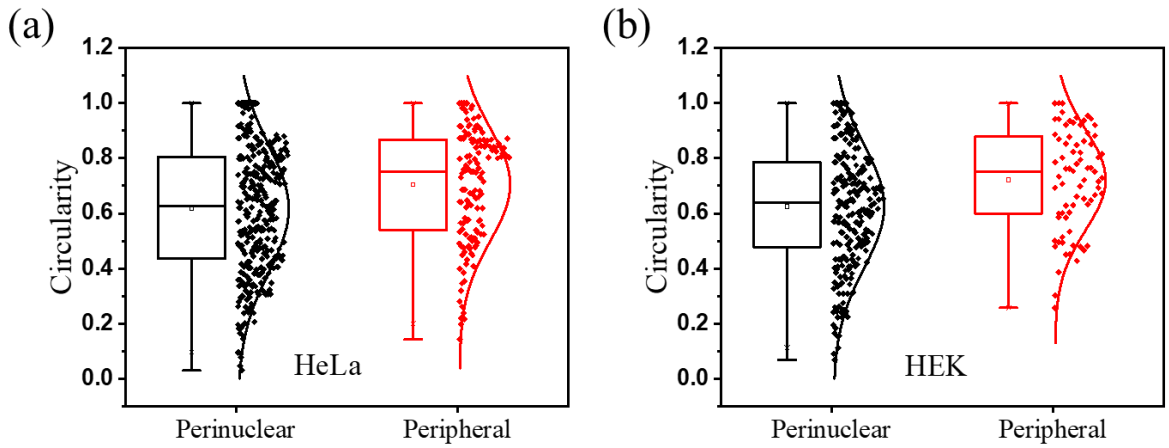

Fig. S15: Morphology of lysosomes at perinuclear and peripheral region: (a and b) represent the morphology of lysosomes in cancerous (HeLa) and non-cancerous cell (HEK) at perinuclear and peripheral region in terms of their circularity. The data in both types of cells show that the lysosomes present at peripheral region are more circular whereas the perinuclear lysosomes are in tubular morphology.

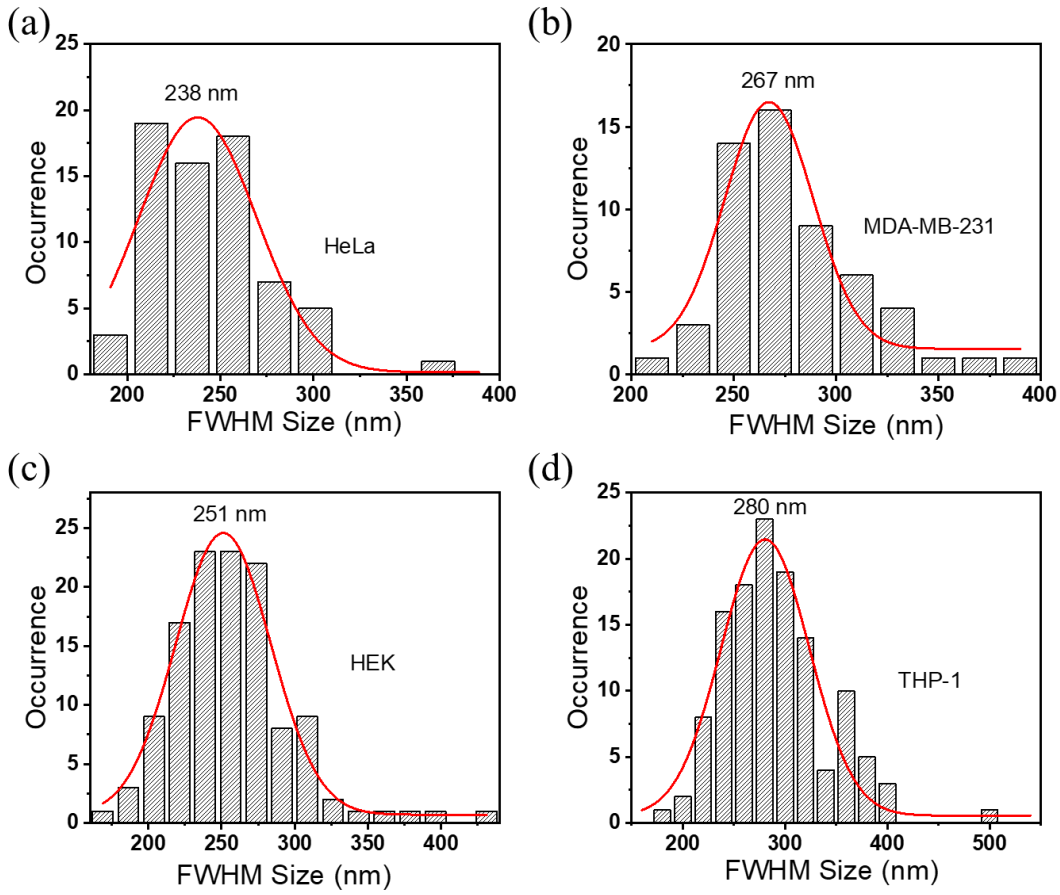

Fig. S16: Size of lysosomes at peripheral position in cancerous and non-cancerous cells: (a and b) represent the histogram of sizes of individual lysosomes in cancerous cells, HeLa and MDA-MB-231, with an average size of 238 nm and 267 nm, respectively. (c and d) show the histogram of individual lysosome size in non-cancerous cells, HEK and THP-1, with an average size of 251 nm and 280 nm, respectively.

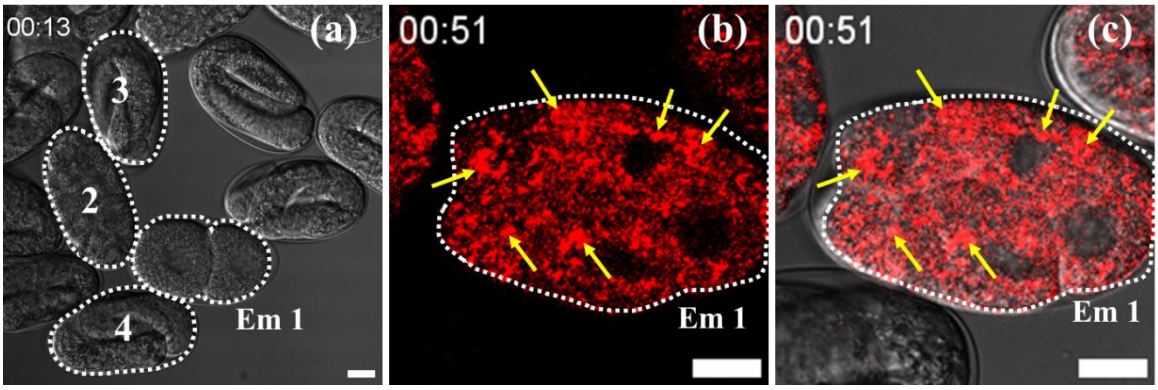

Fig. S17: Embryonic evolution of lysosomes and LROs in *C. elegans* at different stages: (a) TD image of *C. elegans* at 13 minutes (corresponding Zn-complex stained image in **Fig. 7c** shows the disappearance of unstable LROs marked by yellow arrow), (b and c) represent the Zn-complex stained and merge images of Em 1. The data show the increase in LROs number and density (marked as yellow) at around 51 minutes during cell division. Scale bar: 10 µm.